

Crystal structures and magnetic properties of the $RFe_{1-x}Ge_2$ ($R = Gd, Er$) compounds

Mosbah JEMMALI¹, Siwar WALHA¹, Henri NOËL², Rached BEN HASSEN^{1*}

¹ *Unité de Recherche de Chimie des Matériaux, ISSBAT Université de Tunis ElManar
Dr. Zoheir Safi Ave. 9, 1006 Tunis, Tunisia*

² *Laboratoire de Chimie du Solide et Matériaux, Sciences Chimiques de Rennes,
UMR 6226 CNRS-Université Rennes 1, Avenue du Général Leclerc 35042 Rennes, France*

* *Corresponding author. E-mail: rached.benhassen@fss.tru.tn*

Received May 31, 2010; accepted October 29, 2010; available on-line February 15, 2011

In the course of an investigation of solid solutions with $RFe_{1-x}Ge_2$ ($R = Gd, Er$) stoichiometry we have isolated two new phases. Their compositions are $GdFe_{0.37}Ge_2$ and $ErFe_{0.27}Ge_2$, and they have been synthesized by arc melting of pure components and studied by means of X-ray diffraction, SEM analysis and magnetic measurements. They crystallize in the orthorhombic space group $Cmcm$, with defect $CeNiSi_2$ -type structures. Magnetic susceptibility measurements performed in the temperature range 2–300 K showed conventional Curie-Weiss paramagnetic behaviour for both compounds above 25 K. At low temperature, magnetic susceptibility data revealed magnetic phase transitions.

Intermetallic compounds / Chemical synthesis / X-ray diffraction / Electron microscopy

1. Introduction

Ternary $R-Fe-Ge$ systems with $R = Lu, Tm, Er, Ho, Dy, Tb, Gd, Sm, Nd, Pr, Ce,$ and La form a large number of intermetallic compounds [1-3]. Among the numerous compounds reported in the literature corresponding to the composition $RFe_{1-x}Ge_2$, only the structures of $NdFe_{0.45}Ge_2$, $HoFe_{0.33}Ge_2$ and $SmFe_{0.45}Ge_2$ have been determined from single crystal diffraction data [4,5], which confirmed that they crystallize in a defect $CeNiSi_2$ -type crystal structure.

Earlier X-ray powder diffraction studies indicate the existence of the non stoichiometric phases $GdFe_{0.33}Ge_2$ and $ErFe_{0.5}Ge_2$ [6], or $GdFe_{0.46}Ge_2$ and $ErFe_{0.36}Ge_2$ [7], as well as of a few other similar ternary compounds. Structural refinements of $GdFe_{1-x}Ge_2$ and $ErFe_{1-x}Ge_2$ single crystals have not been reported.

While investigating the ternary systems $R-Fe-Ge$ ($R = Gd, Er$) we isolated two new compounds, $GdFe_{0.37}Ge_2$ and $ErFe_{0.27}Ge_2$. This paper reports on the synthesis, crystal structure refinement and magnetic properties of the title compounds.

2. Experimental details

Samples with nominal composition $Gd_3Fe_1Ge_6$ and $Er_3Fe_1Ge_6$, each with a total weight of 0.5 g, were

prepared from high-purity elements (Gd: 99.9%, Er: 99.9%; Ge: 99.9%; Fe 99.8% in mass) by arc-melting under a purified argon atmosphere on a water-cooled copper hearth. The weight losses were less than 1 wt.%. The ingots were annealed in evacuated quartz tubes for 1 week at 800°C and then quenched in cold water.

Scanning electron microscopy (JEOL-JSM 6400) was used to study the microstructure of polished surfaces of the samples. The composition of the phases was analysed by energy-dispersive X-ray spectroscopy (EDX) with an Oxford-Link-Isis Si/Li analyser. The identification of the various phases present in each sample was made by the examination of X-ray powder diffraction data collected using $Co K\alpha_1$ radiation ($\lambda = 1.789007 \text{ \AA}$) (Inel CPS 120 diffractometer).

Single crystal X-ray diffraction experiments were performed on a Nonius Kappa CCD / 95 mm CCD camera. The unit cell parameters were determined and refined during the indexing and intensity integration process of all the recorded image frames, using the program DENZO [8]. Data collection parameters for both compounds are gathered in Table 1.

Magnetic data were collected using a SQUID magnetometer operating in the magnetic field range 0-5 T. Measurements of magnetic susceptibility were made on pieces of bulk samples at temperatures between 2 and 300 K.

Table 1 Crystal data and structure refinement parameters at room temperature.

Compound	$\text{GdFe}_{0.37}\text{Ge}_2$	$\text{ErFe}_{0.27}\text{Ge}_2$
Formula weight (g mol^{-1})	323.1	327.5
Crystal system, space group	orthorhombic, $Cmcm$	orthorhombic, $Cmcm$
a (\AA)	4.1508(2)	4.0790(1)
b (\AA)	16.0609(1)	15.6010(2)
c (\AA)	4.0239(2)	3.9690(1)
V (\AA^3)	268.26(2)	252.573(9)
Z and calculated density (g/cm^3)	4 and 8.00	4 and 8.61
Crystal size (mm^3)	$0.10 \times 0.07 \times 0.04$	$0.04 \times 0.03 \times 0.02$
$F(0\ 0\ 0)$	820	844
Wavelength (\AA)	0.71073 (Mo $K\alpha$)	0.71073 (Mo $K\alpha$)
Diffractometer	Nonius Kappa CCD	Nonius Kappa CCD
Scan method	$2^\circ\Delta\omega$ and $2^\circ\Delta\phi$	$1^\circ\Delta\omega$ and $1^\circ\Delta\phi$
Crystal to detector distance (d) (mm)	25	25
Total frames / expos.time/frame (t) (s)	187 / 60	566 / 90
θ range for data collection ($^\circ$)	2.54-40.15	5.17-41.93
Index ranges	$-7 \leq h \leq 7, -27 \leq k \leq 28,$ $-7 \leq l \leq 7$	$-7 \leq h \leq 7, -28 \leq k \leq 29,$ $-7 \leq l \leq 7$
Reflections collected / unique	841 / 510	890 / 530
Reflections with $I_{\text{obs}} > 2\sigma(I_{\text{obs}})$	446	469
Data / restraints / parameters	510 / 0 / 19	530 / 0 / 19
R_{int} and R_σ	0.0430 and 0.0477	0.0258 and 0.0354
Reliability factor (R_1) ^a	0.0443	0.045
Reliability factor (wR_2) ^b	0.11	0.12
Goodness-of-fit on F^2	1.077	1.051
Extinction coefficient	0.0058(10)	0.0031(9)
Largest diff. peak and hole	5.192 and -5.55 e \AA^{-3}	7.2 and $-6.851 \text{ e \AA}^{-3}$

$$^a R_1 = \frac{\sum |F_o - F_c|}{\sum |F_o|}$$

$$^b wR_2 = \sqrt{\frac{\sum (w(|F_o|^2 - |F_c|^2))^2}{\sum (w|F_o|^2)^2}}$$

3. Results and discussion

3.1. Structure analysis

Single crystals suitable for X-ray measurements were isolated from the samples with nominal composition $\text{Gd}_3\text{Fe}_1\text{Ge}_6$ and $\text{Er}_3\text{Fe}_1\text{Ge}_6$. The crystal data, data collection and refinement details are given in **Table 1**. The structures were solved by the Patterson method and subsequent Fourier analysis [9] and refined by full-matrix least-squares on F^2 of all observed reflections [10]. The final atomic coordinates, occupancies and equivalent displacement parameters are given in **Tables 2** and **3**. Selected interatomic distances in the two compounds are listed in **Table 4**.

The refinements confirm that the two compounds crystallize with the defect CeNiSi_2 structure type. The refinements converged to structural models with the Fe positions not fully occupied. The refined occupancies are 0.37(1) and 0.27(1) for $\text{GdFe}_{1-x}\text{Ge}_2$ and $\text{ErFe}_{1-x}\text{Ge}_2$, respectively, leading to the formulae $\text{GdFe}_{0.37}\text{Ge}_2$ and $\text{ErFe}_{0.27}\text{Ge}_2$. A view of the structure of $\text{GdFe}_{0.37}\text{Ge}_2$ is provided in **Fig. 1**. The Ge atoms form tetragonal pyramids around the Fe atoms; the

pyramids are connected by edges to form the rigid part of the structure in the form of a three-dimensional framework. As shown in **Fig. 2**, the Gd atoms form trigonal prisms around the Ge and Fe atoms. The structure of $R\text{Fe}_{1-x}\text{Ge}_2$ consists of $[\text{Fe}_{1-x}\text{Ge}_2]$ slabs parallel to the ac plane that are held together by zigzag chains of Ge1 atoms aligned along the c direction, forming a three-dimensional framework with channels occupied by R atoms (**Fig. 2**). The unit cell parameters are $a = 4.1508(2) \text{ \AA}$, $b = 16.0609(1) \text{ \AA}$, $c = 4.0239(2) \text{ \AA}$ for $\text{GdFe}_{0.37}\text{Ge}_2$ and $a = 4.0790(1) \text{ \AA}$, $b = 15.6010(2) \text{ \AA}$, $c = 3.9690(1) \text{ \AA}$ for $\text{ErFe}_{0.27}\text{Ge}_2$. As seen in **Table 4**, the Fe–Ge distances (2.175(2)–2.349(5) \AA in $\text{GdFe}_{0.37}\text{Ge}_2$ and 2.131(2)–2.262(5) \AA in $\text{ErFe}_{0.27}\text{Ge}_2$) seem to be anomalously short when compared to typical distances of 2.4–2.5 \AA in Fe–Ge binaries [11,12] or in (Gd,Er) Fe_6Ge_6 [13,14], or to the sum of the metallic radii (2.43 \AA) [15]. Many defect $R\text{M}_{1-x}\text{Ge}_2$ structures [3,4,16] exhibit similar anomalously short M –Ge distances, and in the case of $\text{TbFe}_{0.25}\text{Ge}_2$ [2] a modulated superstructure model was adopted, in which the square Ge net distorts to form cis-trans chains that can accommodate more

Table 2 Atomic coordinates and displacement parameters (\AA^2) for $\text{GdFe}_{0.37}\text{Ge}_2$.

Atom	x	y	z	occ.	U_{eq}	U_{11}	U_{22}	U_{33}	$U_{23}=U_{13}=U_{12}$
Gd	0	0.10326(3)	1/4	1	0.01066(19)	0.00932(3)	0.01054(3)	0.01218(3)	0
Fe	0	0.30304(3)	1/4	0.37(1)	0.0171(12)	0.01911(2)	0.01232(2)	0.02004(2)	0
Ge(1)	0	0.44926(9)	1/4	1	0.0121(2)	0.00951(5)	0.01599(5)	0.01078(5)	0
Ge(2)	0	0.74845(12)	1/4	1	0.0300(4)	0.02910(8)	0.01751(7)	0.04342(10)	0

U_{eq} is defined as one third of the trace of the orthogonalized U_{ij} tensor. The anisotropic displacement factor exponent takes the form: $-2\pi^2 [h^2 a^{*2} U_{11} + \dots + 2hka^*b^* U_{12}]$

Table 3 Atomic coordinates and displacement parameters (\AA^2) for $\text{ErFe}_{0.27}\text{Ge}_2$.

Atom	x	y	z	occ.	U_{eq}	U_{11}	U_{22}	U_{33}	$U_{23}=U_{13}=U_{12}$
Er	0	0.10298(3)	1/4	1	0.01047(18)	0.0101(2)	0.0104(2)	0.0109(2)	0
Fe	0	0.30202(3)	1/4	0.27(1)	0.0099(2)	0.012(2)	0.009(2)	0.009(2)	0
Ge(1)	0	0.44701(11)	1/4	1	0.0282(4)	0.0293(8)	0.0141(6)	0.04131(10)	0
Ge(2)	0	0.74781(10)	1/4	1	0.0134(2)	0.0097(5)	0.021(6)	0.0096(4)	0

U_{eq} is defined as one third of the trace of the orthogonalized U_{ij} tensor. The anisotropic displacement factor exponent takes the form: $-2\pi^2 [h^2 a^{*2} U_{11} + \dots + 2hka^*b^* U_{12}]$

reasonable distances to the capping transition-metal atoms [17]. Attempts to detect a superstructure in the $R\text{Fe}_{1-x}\text{Ge}_2$ compounds studied here were unsuccessful, but it is clear that similar distortions of the square Ge nets are also possible in the title compounds.

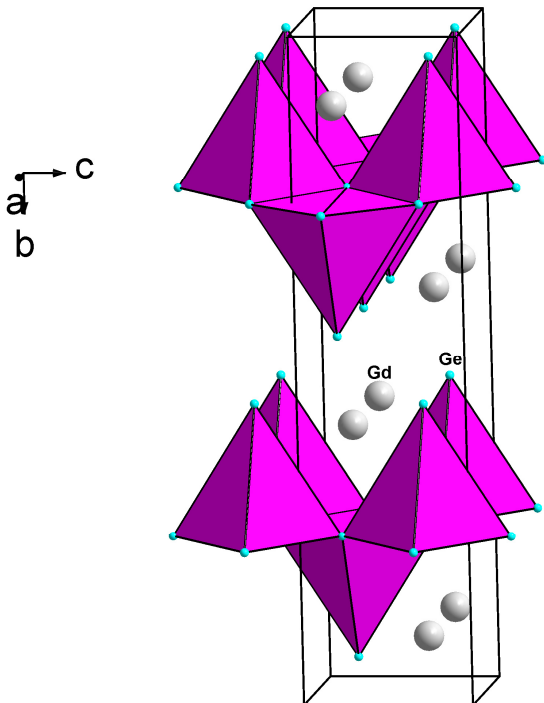


Fig. 1 Perspective view of the structure and coordination polyhedra of the Fe atoms for $\text{GdFe}_{0.37}\text{Ge}_2$.

3.2. Magnetic properties

Figs. 3 and 4 show magnetic susceptibility curves for the $\text{GdFe}_{0.37}\text{Ge}_2$ and $\text{ErFe}_{0.27}\text{Ge}_2$ compounds, respectively, in the temperature range 2-300 K. The temperature dependence of the magnetic susceptibility indicates a magnetic phase transition below 15 K for both compounds. In the paramagnetic state, the magnetic susceptibility of both compounds follows the Curie-Weiss law and can be written:

$$\chi = C / (T - \Theta_p) \quad (1)$$

where Θ_p is the Weiss temperature and C is the Curie constant defined as:

$$C = \frac{\mu_0}{3k_B} \mu_{\text{eff}}^2 \quad (2)$$

where $\mu_0 = 4\pi \cdot 10^{-7} \text{ H m}^{-1}$ is the permeability of vacuum, $k_B = 1.38 \cdot 10^{-23} \text{ J K}^{-1}$ is the Boltzmann constant.

The inverse of the susceptibility in $\mu_0 H = 0.5 \text{ T}$ as a function of temperature is shown in insets of Figs. 3 and 4. By fitting the paramagnetic data to a line in the temperature range 25-300 K, the Curie-Weiss parameters C and Θ_p were obtained. The experimental effective paramagnetic moments, $\mu_{\text{eff}}^{\text{exp}}$, were calculated from C using Eq. (2), and are listed in Table 2 together with C , Θ_p and $\mu_{\text{eff}}^{\text{cal}}$ [18].

For the $\text{GdFe}_{0.37}\text{Ge}_2$ compound, the paramagnetic Weiss temperature $\Theta_p = -36(1) \text{ K}$, the Curie constant $C = 7.78(1) \text{ emu K/mol}$, and the effective paramagnetic moment $\mu_{\text{eff}}^{\text{exp}} = 7.89 \mu_B/\text{mol}$. For the $\text{ErFe}_{0.27}\text{Ge}_2$ compound the paramagnetic Weiss temperature $\Theta_p = -3(1) \text{ K}$, the Curie constant $C = 11.456(3) \text{ emu K/mol}$, and the effective paramagnetic moment $\mu_{\text{eff}}^{\text{exp}} = 9.58 \mu_B/\text{mol}$.

Table 4 Selected interatomic distances (Å) for $\text{GdFe}_{0.37}\text{Ge}_2$ and $\text{ErFe}_{0.27}\text{Ge}_2$.

$\text{GdFe}_{0.37}\text{Ge}_2$		$\text{ErFe}_{0.27}\text{Ge}_2$	
Gd-Ge(1)	3.0111(4) 4×	Er-Ge (1)	2.9506(4) 4 ×
Gd-Ge(2)	3.1178(15) 2×	Er-Ge(2)	3.0439(14) 2×
Gd-Ge(2)	3.1218(14) 2×	Er-Ge(2)	3.0589(14) 2×
Gd-Fe	3.209(5) 1×	Er-Fe	3.105(5) 1×
Gd-Ge(1)	3.2287(11) 2×	Er-Ge(1)	3.1750(13) 2×
Gd-Fe	3.259(2) 4×	Er-Fe	3.209(2) 4×
Gd-Gd	3.879(1) 2×	Er-Er	3.777(1) 2×
Gd-Gd	4.024(1) 2×	Er-Er	3.969(1) 2×
Gd-Gd	4.151(1) 2×	Er-Er	4.079(1) 2×
Fe-Ge(2)	2.175(2) 2×	Fe-Ge(2)	2.131(2) 2×
Fe-Ge(2)	2.253(2) 2×	Fe-Ge(2)	2.208(2) 2×
Fe-Ge(1)	2.349(5) 1×	Fe-Ge(1)	2.262(5) 1×
Fe-Gd	3.209(5) 1×	Fe-Er	3.105(5) 1×
Fe-Gd	3.259(2) 4×	Fe-Er	3.209(2) 4×
Ge(1)-Fe	2.349(5) 1×	Ge(1)-Fe	2.262(5) 1×
Ge(1)-Ge(1)	2.5892(18) 2	Ge(1)-Ge(1)	2.583(2) 2×
Ge(1)-Gd	3.0111(4) 4×	Ge(1)-Er	2.9506(4) 4×
Ge(1)-Gd	3.2287(11) 2×	Ge(1)-Er	3.1750(13) 2×
Ge(2)-Fe	2.175(2) 2×	Ge(2)-Fe	2.131(2) 2×
Ge(2)-Fe	2.253(2) 2×	Ge(2)-Fe	2.208(2) 2×
Ge(2)-Ge(2)	2.89097(12) 4×	Ge(2)-Ge(2)	2.84648(10) 4×
Ge(2)-Gd	3.1178(15) 2×	Ge(2)-Er	3.0439(14) 2×
Ge(2)-Gd	3.1218(14) 2×	Ge(2)-Er	3.0589(14) 2×

Table 5 C , Θ_p , $\mu_{\text{eff}}^{\text{exp}}$ and $\mu_{\text{eff}}^{\text{cal}}$ values for the $\text{GdFe}_{0.37}\text{Ge}_2$ and $\text{ErFe}_{0.27}\text{Ge}_2$ compounds.

Compound	C (emu K/mol)	Θ_p (K)	$\mu_{\text{eff}}^{\text{exp}}$ (μ_B)	$\mu_{\text{eff}}^{\text{cal}}$ (μ_B)
$\text{GdFe}_{0.37}\text{Ge}_2$	7.78696	-36	7.89	7.94
$\text{ErFe}_{0.27}\text{Ge}_2$	11.456	-3	9.58	9.58

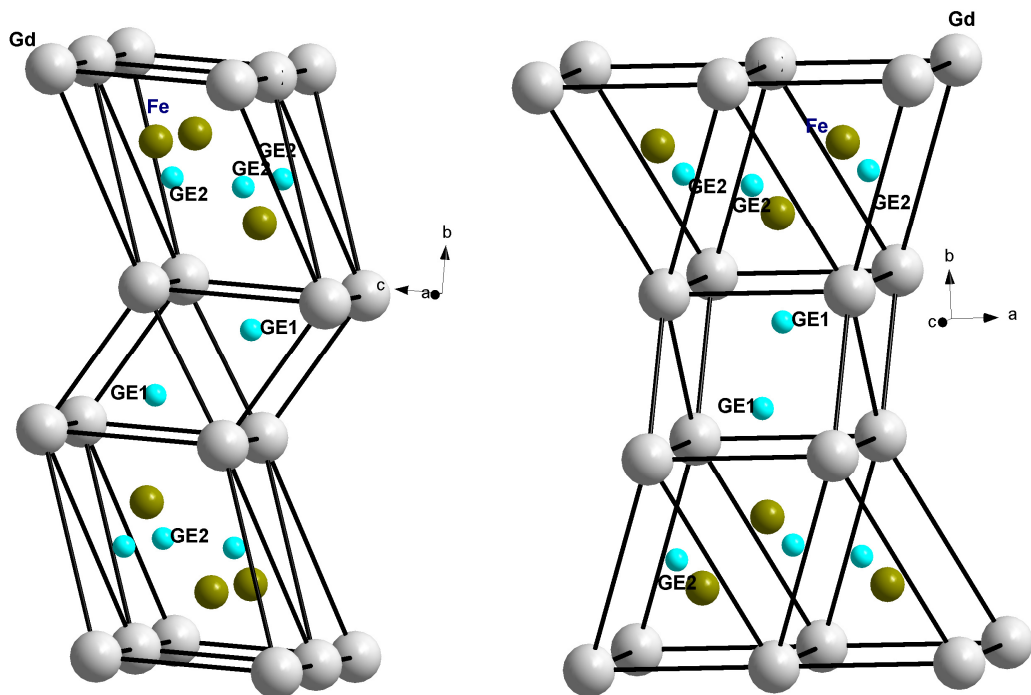


Fig. 2 Arrangement of trigonal prisms in $\text{GdFe}_{0.37}\text{Ge}_2$.

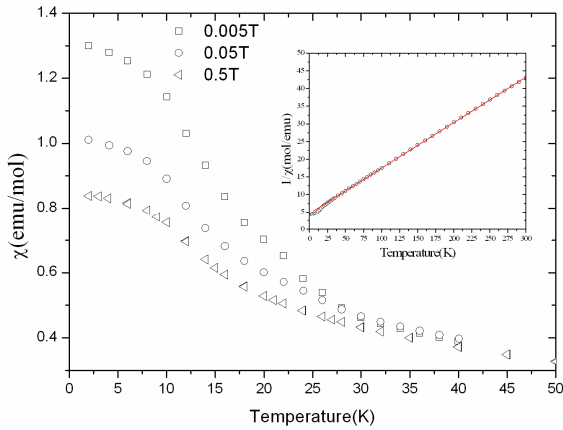


Fig. 3 Temperature dependence of the magnetic susceptibility of $\text{GdFe}_{0.37}\text{Ge}_2$ at various fields. The inset shows the inverse magnetic susceptibility of $\text{GdFe}_{0.37}\text{Ge}_2$ measured in a field of 0.5 T; the solid line is the fit to the Curie-Weiss behavior.

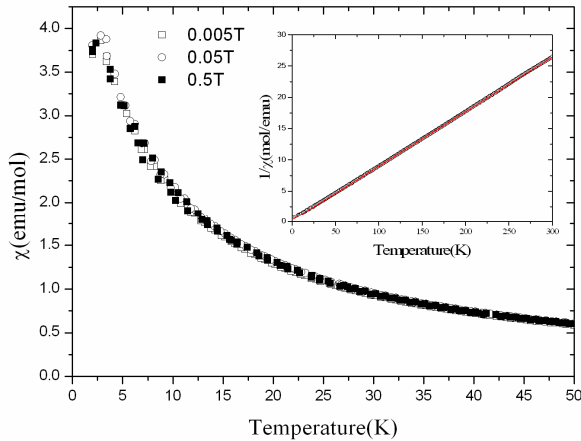


Fig. 4 Temperature dependence of the magnetic susceptibility of $\text{ErFe}_{0.27}\text{Ge}_2$ at various fields. The inset shows the inverse magnetic susceptibility of $\text{ErFe}_{0.27}\text{Ge}_2$ measured in a field of 0.5 T; the solid line is the fit to the Curie-Weiss behavior.

The effective paramagnetic moments of the $\text{GdFe}_{0.37}\text{Ge}_2$ ($7.89 \mu_B/\text{mol}$) and $\text{ErFe}_{0.27}\text{Ge}_2$ ($9.58 \mu_B/\text{mol}$) compounds are in agreement with a contribution of Gd^{3+} and Er^{3+} ions only, suggesting that the Fe atoms do not carry localized magnetic moments. The low-temperature magnetic susceptibility data measured in different fields exhibit for the $\text{ErFe}_{0.27}\text{Ge}_2$ compound (Fig. 4) an increase below 12 K and a peak at 3 K. In contrast to the $\text{ErFe}_{0.27}\text{Ge}_2$ compound, the magnetic susceptibility of $\text{GdFe}_{0.37}\text{Ge}_2$ is field-dependent (Fig. 3) with a similar shape of the temperature dependence and a plateau below 12 K in a relatively low field (0.05 T). Such a behavior of the magnetic susceptibility is typical for a ferrimagnetic system. However, the two-sublattice

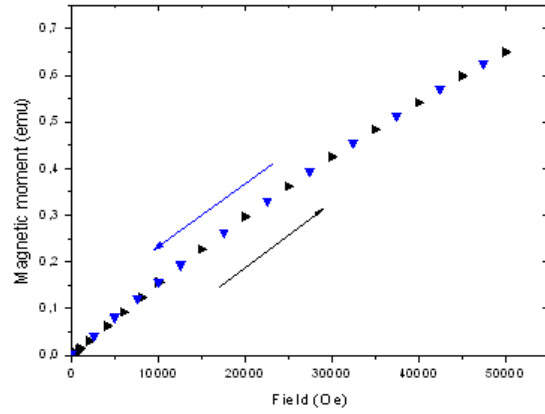


Fig. 5 Isothermal magnetization of $\text{GdFe}_{0.37}\text{Ge}_2$ as a function of magnetic field measured at 2 K.

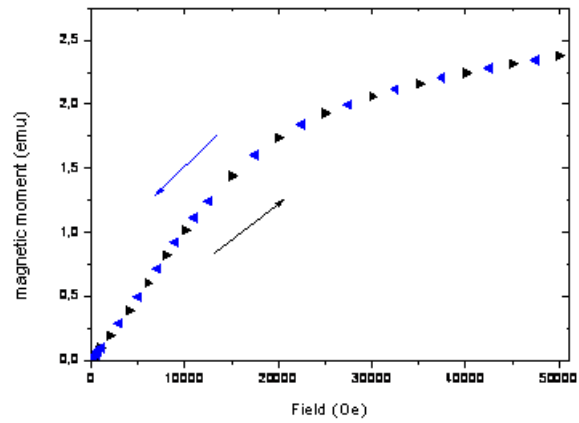


Fig. 6 Isothermal magnetization of $\text{ErFe}_{0.27}\text{Ge}_2$ as a function of magnetic field measured at 2 K.

model of ferrimagnetism requires two types of moment-contributing atom, whereas the values of the effective moments ($\mu_{\text{eff}}^{\text{exp}} = 7.89 \mu_B/\text{mol}$ for $\text{GdFe}_{0.37}\text{Ge}_2$, $\mu_{\text{eff}}^{\text{exp}} = 9.58 \mu_B/\text{mol}$ for $\text{ErFe}_{0.27}\text{Ge}_2$) clearly indicate that only Gd and Er atoms carry moments and there is no moment on Fe atoms. This rules out the possibility of a ferrimagnetic transition in $\text{GdFe}_{0.37}\text{Ge}_2$ and $\text{ErFe}_{0.27}\text{Ge}_2$. A similar behavior was observed by Anupam *et al.* in $\text{Pr}_2\text{Pd}_3\text{Si}_5$ [19]. The field dependence of the isothermal magnetization at 2 K (Figs. 5 and 6) shows that the magnetization increases almost linearly with increasing field for $\text{GdFe}_{0.37}\text{Ge}_2$, but in the case of the $\text{ErFe}_{0.27}\text{Ge}_2$ compound it rises rapidly in low fields (2 T) and then increases almost linearly with increasing field. It is difficult to attribute the weak nonlinearity observed in the magnetization data at 2 K for this compound to the presence of short-range correlations. Future experiments are planned to clarify this behavior.

References

- [1] P. Salamakha, M. Konyk, O. Sologub, O.I. Bodak, *J. Alloys Compd.* 234 (1996) 151-156.
- [2] M. François, G. Venturini, B. Malaman, B. Roques, *J. Less-Common Met.* 160 (1990) 197-213.
- [3] V.K. Pecharsky, O.Ya. Mruz, M.B. Konyk, P.S. Salamakha, P.K. Starodub, M.F. Fedyna, O.I. Bodak, *Zh. Strukt. Khim.* 30(5) (1989) 96.
- [4] L. Zeng, H.F. Franzen, *J. Alloys Compd.* 267 (1998) 86-89.
- [5] O.I. Bodak, O.Ya. Mruz, V.K. Pecharskii, *Izv. Akad. Nauk SSSR, Neorg. Mater.* 26(4) (1990) 773-775.
- [6] V.K. Pecharskii, O.Y. Mrooz, M.B. Konyk, P.S. Salamakha, P.K. Starodub, M.F. Fedyna, O.I. Bodak, *Zh. Strukt. Khim.* 30 (1989) 777-782.
- [7] M. Francois, G. Venturini, B. Malaman, B. Roques, *J. Less-Common. Met.* 160 (1990) 197-213.
- [8] *Nonius Kappa CCD Program Package*, Nonius, Delft, The Netherlands, 1998.
- [9] G.M. Sheldrick, *Program for the Solution of Crystal Structures*, University of Göttingen, Germany, 1985.
- [10] G.M. Sheldrick, *Program for Crystal Structure Refinement*, University of Göttingen, Germany, 1997.
- [11] H. Watanabe, N. Kunitomi, *J. Phys. Soc. Jpn.* 21 (1966) 1932-1935.
- [12] M. Richardson, *Acta Chem. Scand.* 21 (1967) 2305-2317.
- [13] O.Y. Mruz, P.K. Starodub, O.I. Bodak, *Dopov. Akad. Nauk Ukr. RSR, Ser. B* (12) (1984) 44.
- [14] O. Oleksyn, P. Schobinger Papamantellos, J. Rodriguez Carvajal, E. Brück, K.H.J. Buschow, *J. Alloys Compd.* 257 (1997) 36-45.
- [15] L. Pauling, *The Nature of the Chemical Bond*, 3rd Ed., Cornell University Press, Ithaca, NY, 1960.
- [16] H. Bie, A.V. Tkachuk, A. Mar, *J. Solid State Chem.* 182 (2009) 122-128.
- [17] M.A. Zhuravleva, D. Bilc, R.J. Pcionek, S.D. Mahanti, M.G. Kanatzidis, *Inorg. Chem.* 44 (2005) 2177-2188.
- [18] K.H.J. Buschow, In: E.P. Wohlfarth (Ed.), *Ferromagnetic Materials*, Vol. 1, North Holland Publishing Company, Amsterdam, 1980.
- [19] Anupam, V.K. Anand, V. Ganesan, Z. Hossain, *J. Magn. Magn. Mater.* 321 (2009) 2753-2756.

Proceeding of the XI International Conference on Crystal Chemistry of Intermetallic Compounds, Lviv, May 30 - June 2, 2010.